Preprints of the 18th IFAC World Congress
Milano (Italy) August 28 - September 2, 2011

Weight optimization for maximizing robust performance in $\mathscr{H}_\infty$ loop-shaping design

M. Osinuga * **S. Patra** * **A. Lanzon** *

* *Control Systems Centre, University of Manchester, Manchester, United Kingdom. M13 9PL.*

Abstract: This paper proposes a design framework that maximizes the robust performance of a closed-loop system via weight optimization in $\mathscr{H}_\infty$ loop-shaping control. In line with design objectives, frequency-dependent optimization problems are formulated in LMI framework to maximize robust performance at low and high frequencies, and directly improve the robust stability margin at mid frequencies. The philosophy of the work thus gives the best robust performance that can be achieved on a particular problem once a level of robust stability margin is demanded. Loop-shaping weights and controller are simultaneously synthesized from the proposed algorithm.

Keywords: $\mathscr{H}_\infty$ loop-shaping; Performance; Robustness; Weight optimization; Robust control.

1. INTRODUCTION

The $\mathscr{H}_\infty$ loop-shaping design procedure (LSDP) McFarlane and Glover [1992] is a well-known robust design methodology that establishes a good trade-off between the robust stability and the robust performance of a closed-loop system (see McFarlane and Glover [1992] for more information). In this design framework, the achieved robust stability margin is a design indicator and thus, a designer's main task is to select "good" weights that achieve large robust stability margin. A robust stability margin of 0.3 is typically considered satisfactory in most control system design as it corresponds to a closed-loop system's gain and phase margins greater than or equal to 5.39dB and 34.92°, respectively, Glover et al. [2000].

It is however known that the selection of weights is non-trivial especially for plants with strong coupling Tsai et al. [1990], McFarlane and Glover [1992], Hyde [1995], Papageorgiou and Glover [1997], Lanzon [2005], and factors such as the right-half plane (RHP) poles/zeros of the nominal plant, strength of cross-coupling for multi-input multi-output (MIMO) systems, roll-off rate around crossover, expected bandwidth, singular values and condition numbers of the nominal plant, etc. must be duly considered when selecting weights. These issues have been discussed in McFarlane and Glover [1992], Zhou et al. [1996], Papageorgiou and Glover [1997], Lanzon [2005]. Moreover, the factors have been combined in Lanzon [2005] into a single optimization framework that facilitates design via an algorithm that simultaneously synthesizes weights and a stabilizing controller while maximizing the robust stability margin for a given performance. Furthermore, smoothness constraints, formulated on the gradient of weights, have been incorporated as extension of this work in Osinuga et al. [2010a,b]. This allows fitting by low-order transfer functions and also facilitates the synthesis of smooth weights, thereby extending the applicability of the algorithm to lightly damped or undamped plants without the undesirable lightly-damped 'approximate' pole-zero cancelations in the shaped plant.

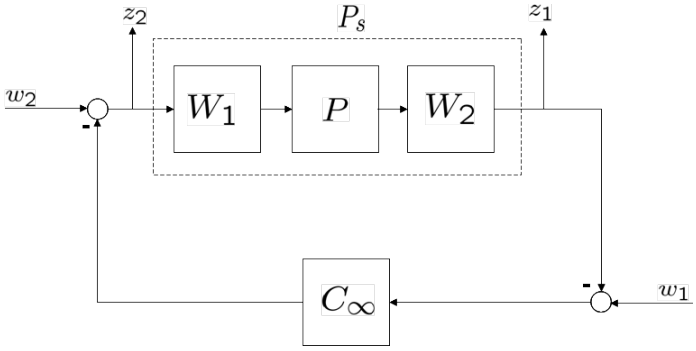

Figure 1. Feedback interconnection

There has been a lot of interest in relating the best achievable performance level in a feedback control system for different plant characteristics, e.g., relationship between phase property of the plant and the achievable control performance in $\mathscr{H}_\infty$ LSDP Hara et al. [2006], performance bounds for the $\mathscr{H}_\infty$-optimal control of discrete linear time-invariant stable scalar plants Peters and Salgado [2009], etc. However, the paradigms of the optimization problem described above and, in fact, many other synthesis techniques do not yield a synthesis framework for the best achievable performance for a given plant because the objective is solely to maximize the robust stability margin for a given performance.

In order to answer the question of the achievable performance of a closed-loop system, an approach that combines performance with robust stability objectives at appropriate frequency regions that are based on design objectives is needed. We therefore propose an optimization problem that prioritizes performance, stability and robustness at low, mid and high frequencies, respectively. The resulting performance bound from this optimized approach provides designers with a general feel of the performance level that can be achieved when a desired level of robust stability margin is demanded. This framework is relevant as there are many scenarios where performance

⋆ The financial support of the Engineering and Physical Sciences Research Council and the Royal Society is gratefully acknowledged. Corresponding author M. Osinuga (e-mail: mobolaji.osinuga-2@postgrad.manchester.ac.uk. Tel. +44(0)161-306-2821. Fax +44-161-306-9341.)

requirements are so stringent in the design that they have to be optimized, e.g., performance of modern high-maneuverable aircrafts and long-range missiles is critical once the stability of the system is guaranteed Min et al. [2007].

The philosophy of this work casts a frequency-dependent optimization problem that improves the robust stability margin around crossover frequency and, for a guaranteed level of robust stability margin, maximizes both robust performance at low frequencies and robustness to unmodeled dynamics and unpredicted sensor noise, etc. at high frequencies. The resulting solution algorithm simultaneously synthesizes a robust stabilizing controller and loop-shaping weights in a systematic framework that is easy for designers to use. The proposed optimization problem builds on the framework established in Lanzon [2005], Osinuga et al. [2010a,b].

The rest of the paper is organized as follows: notations that are central to subsequent sections are defined in Section II and some preliminaries on $\mathscr{H}_\infty$ LSDP's concept and the extended weight optimization framework of Lanzon [2005], Osinuga et al. [2010b] are stated in Section III. The optimization problem for maximizing the robust performance and its solution are established in Sections IV and V, respectively. An illustrative example is given in Section VI and the conclusion is stated in Section VII.

2. NOTATIONS

Let $\mathbb{R}, \mathbb{R}_+, \mathbb{R}_+^n$ respectively denote the set of real numbers, strictly positive real numbers and column vectors of dimension $(n\times 1)$, with each entry belonging to $\mathbb{R}_+$. $\mathscr{R}^{n\times m}$ and $\mathscr{RH}_\infty^{n\times m}$ are the set of real rational and real rational stable transfer function matrices, respectively, each of dimension $(n\times m)$. Functions that are units in $\mathscr{RH}_\infty$ are said to belong to $\mathscr{GH}_\infty$, i.e., $f \in \mathscr{GH}_\infty \Leftrightarrow f, f^{-1} \in \mathscr{RH}_\infty$.

$\text{diag}\begin{pmatrix} a \\ b \end{pmatrix}$ is a shorthand notation for $\begin{pmatrix} a & 0 \\ 0 & b \end{pmatrix}$.

Let $\mathbf{\Lambda_n} := \{\text{diag}(x) : x \in \mathbb{R}_+^n\}$ be the set of real strictly positive diagonal matrices of dimension $(n\times n)$. Also, let $\mathscr{C}(P)$ denote the set of all stabilizing controllers for a plant P. For matrix A, the i-th singular value is represented as $\sigma_i(A)$ and the condition number is defined as $\kappa(A) := \overline{\sigma}(A)/\underline{\sigma}(A)$, where $\overline{\sigma}(A)$ (resp. $\underline{\sigma}(A)$) is the largest (resp. smallest) singular value. A^* is the complex conjugate transpose of matrix A. The robust stability margin $b(P_s, C_\infty)$ of the feedback interconnection shown in Figure 1 is defined as

$$b(P_s,C_\infty) := \left\| \begin{bmatrix} P_s \\ I \end{bmatrix} (I - C_\infty P_s)^{-1} \begin{bmatrix} -C_\infty & I \end{bmatrix} \right\|_\infty^{-1} \tag{1}$$

if $C_\infty \in \mathscr{C}(P)$, otherwise 0. The maximum achievable robust stability margin $b_{opt}(P_s) := \sup_{C_\infty} b(P_s, C_\infty) \in [0,1]$. We denote γ as $b(P_s, C_\infty)^{-1}$ and the pointwise-in-frequency robust stability margin at a frozen frequency ω is defined as $\rho_\omega(P_s, C_\infty) := b(P_s(j\omega), C_\infty(j\omega))$, where $C_\infty = W_1^{-1} C W_2^{-1}$. The following set is defined for compactness of notation:

$$\mathbf{\Pi}(\alpha,\beta,\zeta,\eta) := \{W = \text{diag}\begin{pmatrix} w_1 \\ \vdots \\ w_p \end{pmatrix} \in \mathscr{GH}_\infty^{p\times p} : \alpha(\omega) < \sigma_i(W(j\omega)) < \beta(\omega), \kappa(W(j\omega)) < \zeta(\omega),$$
$$\left| \frac{d}{d(\log_{10}\omega)} (20\log_{10}|w_i(j\omega)|) \right| < \eta(\omega)\ \forall \omega, i = 1,\ldots,p\}$$ for some given continuous frequency functions α, β, ζ, $\eta : \mathbb{R} \to \mathbb{R}_+$ that satisfy $\beta(\omega) > \alpha(\omega), \zeta(\omega) > 1$ and $\eta(\omega) > 0\ \forall\omega$. For W, α and β delimit the allowable region for the singular values, ζ provides a bound for the condition number and η, expressed in dB/decade, provides bound for the gradient of the magnitude response of the diagonal elements. For a given scaled plant $P \in \mathscr{R}^{m\times n}$, further define
$\Lambda_{1\omega} := W_1(j\omega)^{-*} W_1(j\omega)^{-1} \in \mathbf{\Lambda_n}$ and
$\Lambda_{2\omega} := W_2(j\omega)^* W_2(j\omega) \in \mathbf{\Lambda_m}$.

3. $\mathscr{H}_\infty$ LSDP AND WEIGHT OPTIMIZATION FRAMEWORK

Here, the extended weight optimization framework of Lanzon [2005] and some concepts of the $\mathscr{H}_\infty$ LSDP are described for underpinning the concepts and mathematical machinery of this work. Typically, loop-shaping weights W_1 and W_2 are chosen to shape the singular values of the nominal plant P such that the shaped plant P_s has large gain at low frequencies, small gain at high frequencies and does not roll off at a high rate around crossover. We denote ω_l and ω_u as the boundary frequencies used to partition the frequency space into three distinct frequency regions of low, mid and high frequencies, respectively. A prior knowledge on disturbance characteristics, modeling uncertainties, sensor noise, etc. is needed to choose these boundary frequencies. However, a simple rule [1] of thumb can be made as follows: $\omega_l = 0.1\omega_B$ and $\omega_u = 10\omega_B$, where ω_B is the desired bandwidth.

Besides achieving the desired loop-shape, a designer must also ensure that a number of standard closed-loop design objectives discussed in McFarlane and Glover [1992], Zhou et al. [1996], Lanzon [2005] are small in appropriate frequency ranges. Bounds on the transfer functions representing these objectives are specified in terms of the singular values of the shaped plant, the robust stability margin and the singular values and condition numbers of the weights. The constraints on the singular values and condition numbers of the loop-shaping weights must therefore be enforced at all frequencies so as to constrain the bounds on these transfer functions at all frequencies.

The extended weight optimization framework of Lanzon [2005] in Osinuga et al. [2010b] captures the above concepts in a systematic framework. The algorithm includes smoothness constraints on the gradient of the loop-shaping weights in addition to existing constraints of Lanzon [2005]. The resulting solution algorithm facilitates the synthesis of smooth weights for lightly-damped plants without the undesirable 'approximate' pole-zero cancelation of the modes of the nominal plant when the shaped plant is formed. The optimization problem in Osinuga et al. [2010b] was posed as follows:

$$\begin{array}{ll} \max & b_{opt}(P_s) \\ W_1 \in \mathbf{\Pi}(\underline{w}_1, \overline{w}_1, k_1, g_1) & \\ W_2 \in \mathbf{\Pi}(\underline{w}_2, \overline{w}_2, k_2, g_2) & \end{array}$$

$$\text{subject to } \underline{s}(\omega) < \sigma_i(P_s(j\omega)) < \overline{s}(\omega)\ \forall i, \omega.$$

$\underline{s}, \overline{s}, \underline{w}_i, \overline{w}_i, k_i$ and g_i are frequency functions specified by the designer for loop-shaping weight $W_i(j\omega)$ $(i = 1,2)$; the region between $\underline{s}$ and $\overline{s}$ represents the permissible region for the desired loop-shape, and is selected based on performance specification. The above optimization problem seeks to maximize

[1] When using this rule, some allowances must be incorporated such that the desired objectives (in frequency) are not too close to ω_l and ω_u due to contrasting design objectives around these boundary frequencies.

$b_{opt}(P_s)$ and therefore does not depend on any particular controller. Using the definition of $b(P_s, C_\infty)$ in (1) and performing several algebraic manipulations, the optimization problem was formulated at each frequency grid-point ω_q, where $q = 1, 2, \ldots, N$ and N is selected by the designer and $\delta\nu := \log_{10}\omega_q - \log_{10}\omega_{q-1}\ \forall q > 1$:

Minimize $\gamma^2_{\omega_q}$
such that $\exists C \in \mathscr{C}(P), \Lambda_{1\omega_q} \in \mathbf{\Lambda_n}, \Lambda_{2\omega_q} \in \mathbf{\Lambda_m}$
satisfying

$$\underline{s}(\omega_q)^2 \Lambda_{1\omega_q} < P^*(j\omega_q)\Lambda_{2\omega_q}P(j\omega_q), \tag{2a}$$

$$P^*(j\omega_q)\Lambda_{2\omega_q}P(j\omega_q) < \overline{s}(\omega_q)^2\Lambda_{1\omega_q}, \tag{2b}$$

$$\begin{aligned}&\begin{bmatrix} 0 & P(j\omega_q) \\ 0 & I \end{bmatrix}^* \begin{bmatrix} \Lambda_{2\omega_q} & 0 \\ 0 & \Lambda_{1\omega_q} \end{bmatrix} \begin{bmatrix} 0 & P(j\omega_q) \\ 0 & I \end{bmatrix} \\ &\leq \gamma^2_{\omega_q} \begin{bmatrix} I & P(j\omega_q) \\ C(j\omega_q) & I \end{bmatrix}^* \begin{bmatrix} \Lambda_{2\omega_q} & 0 \\ 0 & \Lambda_{1\omega_q} \end{bmatrix} \times \ldots \\ &\ldots \times \begin{bmatrix} I & P(j\omega_q) \\ C(j\omega_q) & I \end{bmatrix},\end{aligned} \tag{2c}$$

$$\exists \underline{\xi}_{1\omega_q}, \overline{\xi}_{1\omega_q} : \underline{\xi}_{1\omega_q} I < \Lambda_{1\omega_q} < \overline{\xi}_{1\omega_q} I, \overline{w}_1(\omega_q)^{-2} < \underline{\xi}_{1\omega_q},$$

$$\overline{\xi}_{1\omega_q} < \underline{w}_1(\omega_q)^{-2},\ \overline{\xi}_{1\omega_q} < k_1(\omega_q)^2 \underline{\xi}_{1\omega_q}, \tag{2d}$$

$$\exists \underline{\xi}_{2\omega_q}, \overline{\xi}_{2\omega_q} : \underline{\xi}_{2\omega_q} I < \Lambda_{2\omega_q} < \overline{\xi}_{2\omega_q} I, \underline{w}_2(\omega_q)^2 < \underline{\xi}_{2\omega_q},$$

$$\overline{\xi}_{2\omega_q} < \overline{w}_2(\omega_q)^2,\ \overline{\xi}_{2\omega_q} < k_2(\omega_q)^2 \underline{\xi}_{2\omega_q}, \tag{2e}$$

$$0 < \begin{bmatrix} \frac{\ln 10}{10}\Lambda_{1\omega_{q-1}} g_1(\omega_q)\,\delta\nu & \left(\Lambda_{1\omega_q} - \Lambda_{1\omega_{q-1}}\right) \\ \left(\Lambda_{1\omega_q} - \Lambda_{1\omega_{q-1}}\right) & \frac{\ln 10}{10}\Lambda_{1\omega_{q-1}} g_1(\omega_q)\,\delta\nu \end{bmatrix}, \tag{2f}$$

$$0 < \begin{bmatrix} \frac{\ln 10}{10}\Lambda_{2\omega_{q-1}} g_2(\omega_q)\,\delta\nu & \left(\Lambda_{2\omega_q} - \Lambda_{2\omega_{q-1}}\right) \\ \left(\Lambda_{2\omega_q} - \Lambda_{2\omega_{q-1}}\right) & \frac{\ln 10}{10}\Lambda_{2\omega_{q-1}} g_2(\omega_q)\,\delta\nu \end{bmatrix}. \tag{2g}$$

Note that (2f)-(2g) are only active after the first grid-point optimization, i.e., $q > 1$ in this case. The above optimization problem is quasiconvex when the controller $C \in \mathscr{C}(P)$ is held fixed. Diagonal weights are considered in the above optimization, which is in line with the observation that diagonal loop-shaping weights are generally sufficient to shape the singular values of the nominal plant Hyde [1995]. However, with minor modifications as discussed in Lanzon [2005], it is easy to compute non-diagonal weights. Here, (2a)-(2b) delimit the singular values of the shaped plant P_s within the specified loop-shape boundaries $\underline{s}(\omega_q)$ and $\overline{s}(\omega_q)$ and (2c) captures the cost function that maximizes $b(P_s, C_\infty)$. In addition, (2d)-(2e) provide bounds on the singular values and condition numbers of the synthesized loop-shaping weights while (2f)-(2g) ensure the smoothness in the magnitude response of W_i by restricting the gradient at each frequency grid-point ω_q w.r.t. ω_{q-1} within specified bounds $g_i(\omega_q)\ \forall i = 1, 2$.

4. FRAMEWORK FOR MAXIMIZING ROBUST PERFORMANCE

Now, based on the design objectives, a new optimization problem is formulated to maximize the robust performance using the framework given in (2a)-(2g) without introducing any form of conservatism. The objectives are divided into three parts for the low, mid and high frequency regions as stated below.

(1) $\forall \omega < \omega_l$: maximize the robust performance which is captured by the loop-gain of the shaped plant P_s;
(2) $\forall \omega \in [\omega_l, \omega_u]$: maximize $b(P_s, C_\infty)$ without restricting the loop-shape;
(3) $\forall \omega > \omega_u$: maximize the robustness to high frequency noises, disturbances and unmodeled dynamics by minimizing the loop-gain of the shaped plant P_s.

The desired level of robust stability margin for (1) and (3) above is chosen 'a priori' and denoted as $\bar{\epsilon} \in (0, 1)$.

4.1 Optimization in the low frequency region

In this frequency region, a designer seeks to maximize the loop-gain in order to obtain small sensitivity function for good reference tracking capabilities and good output disturbance rejection. This is captured via the following optimization problem.
Given $\bar{\epsilon}$, P and $C \in \mathscr{C}(P)$, at each $\omega < \omega_l$, solve:

$$\begin{aligned} &\max && \underline{s}(\omega) \\ &W_1 \in \mathbf{\Pi}(\underline{w}_1, \overline{w}_1, k_1, g_1) \\ &W_2 \in \mathbf{\Pi}(\underline{w}_2, \overline{w}_2, k_2, g_2) \end{aligned}$$

subject to
(i) $\underline{s}(\omega) < \sigma_i(P_s(j\omega))\ \forall i$, (ii) $\bar{\epsilon} < \rho_\omega(P_s(j\omega), C_\infty(j\omega))$.
This problem can be recast into the following pointwise-in-frequency quasiconvex optimization problem.
Given $\bar{\epsilon}$, P and $C \in \mathscr{C}(P)$, at each $\omega_q < \omega_l$, solve:

Minimize $\underline{s}(\omega_q)^{-2}$
such that $\exists \Lambda_{1\omega_q} \in \mathbf{\Lambda_n}, \Lambda_{2\omega_q} \in \mathbf{\Lambda_m}$ satisfying (2a), (2c)-(2g), where γ_{ω_q} is fixed at $\bar{\epsilon}^{-1}$ in (2c).
(2b) is not included in this optimization problem as the loop-gain is being maximized from below.

4.2 Optimization in the mid frequency region

The robust stability margin indicates the size of the largest $\mathscr{H}_\infty$-norm bounded perturbation of the normalized coprime factors of the shaped plant P_s for which closed-loop stability is guaranteed [Vinnicombe, 2001, Theorem 1.20]. Hence, the pointwise-in-frequency robust stability margin is maximized in this region without worrying about performance, i.e., maximizing the gain and phase margins so as to avoid a perturbed plant encircling the Nyquist point. The roll-off rate of the shaped plant around the crossover frequency will effectively be constrained as the robust stability margin is maximized.

Given P and $C \in \mathscr{C}(P)$, the optimization problem is cast as follows:

$$\begin{aligned} &\max && \rho_\omega(P_s(j\omega), C_\infty(j\omega)) \\ &W_1 \in \mathbf{\Pi}(\underline{w}_1, \overline{w}_1, k_1, g_1) \\ &W_2 \in \mathbf{\Pi}(\underline{w}_2, \overline{w}_2, k_2, g_2) \end{aligned}$$

at each frequency $\omega \in [\omega_l, \omega_u]$.
The above problem can be recast into the following quasiconvex optimization problem at each $\omega_q \in [\omega_l, \omega_u]$.
Given P and $C \in \mathscr{C}(P)$, solve:

Minimize $\gamma^2_{\omega_q}$
such that $\exists \Lambda_{1\omega_q} \in \mathbf{\Lambda_n}, \Lambda_{2\omega_q} \in \mathbf{\Lambda_m}$ satisfying LMI constraints (2c)-(2g).

In this frequency region, LMI constraints (2a)-(2b) are not included as robust stability is prioritized over nominal performance.

4.3 Optimization in the high frequency region

The aim in this frequency region is to minimize the loop-gain of the compensated system in order to obtain small complementary sensitivity function for good robustness to high frequency unmodeled dynamics and good high frequency sensor noise rejection. This is captured via the following optimization problem.
Given $\bar{\epsilon}$, P and $C \in \mathscr{C}(P)$, at each $\omega > \omega_u$, solve:

$$\begin{array}{ll} \min & \overline{s}(\omega) \\ W_1 \in \mathbf{\Pi}(\underline{w}_1, \overline{w}_1, k_1, g_1) & \\ W_2 \in \mathbf{\Pi}(\underline{w}_2, \overline{w}_2, k_2, g_2) & \end{array}$$

subject to
(i) $\sigma_i(P_s(j\omega)) < \overline{s}(\omega)\ \forall i$, (ii) $\bar{\epsilon} < \rho_\omega(P_s(j\omega), C_\infty(j\omega))$.
This can be similarly cast into the following pointwise-in-frequency quasiconvex optimization problem.
Given $\bar{\epsilon}$, P and $C \in \mathscr{C}(P)$, at each $\omega_q > \omega_u$, solve:

Minimize $\overline{s}(\omega_q)$[2]
such that $\exists \Lambda_{1\omega_q} \in \mathbf{\Lambda_n}, \Lambda_{2\omega_q} \in \mathbf{\Lambda_m}$ satisfying LMI constraints (2b)-(2g) with γ_{ω_q} fixed at $\bar{\epsilon}^{-1}$ in (2c).
(2a) is not included as the loop-gain is being minimized from above.

The above formulations maximize performance, stability and robustness at low, mid and high frequencies, respectively. The formulations are quasiconvex when the stabilizing controller $C \in \mathscr{C}(P)$ is held fixed, and can be easily solved using LMI routines, for example, '*gevp*' solver in MATLAB LMI toolbox. Note that the constraints on the singular values, the condition numbers and the gradients of the loop-shaping weights are active at all frequencies.

5. SOLUTION ALGORITHM

Based on the formulations given in the previous section, a sub-optimal solution algorithm is now proposed. An iterative algorithm must be used to solve the posed problems since they are not simultaneously convex in all variables. Moreover, since there are three optimization problems to be solved, a systematic procedure must be employed such that there is no discontinuity or violation of constraints. In fact, the following should be noted.

(1) Designers typically use W_1 and W_2 to alter the loop-gain at low and high frequencies, respectively Skogestad and Postlethwaite [1998]. We will follow this general design practice by keeping W_2 and W_1 fixed in low and high frequencies, respectively.
(2) Since robust stability can easily be lost near crossover frequency Vinnicombe [2001], we will solve the mid frequency optimization problem before solving the low and high frequency optimization problems. Also, the low and high frequency optimizations will use the boundary values obtained in the mid frequency optimization to seed their search in order to avoid discontinuity and violation of constraints at the boundaries of the frequency regions.
(3) The magnitude values of the weights at ω_l and ω_u will be constrained by the magnitude values of the weights obtained at these frequencies in the previous iteration due to contrasting design objectives at these boundary frequencies, e.g. at $\omega_q = \omega_l$, we maximize $\rho_{\omega_q}(P_s, C_\infty)$ while at ω_{q-1}, we maximize $\underline{s}(\omega_{q-1})$ for a fixed $\bar{\epsilon}$. This constraint is needed to ensure monotonic improvement in performance in low frequencies and robustness in high frequencies.

The following quantities need to be specified as inputs to the algorithm: a scaled nominal plant $P \in \mathscr{R}^{m\times n}$, where [2] $m \geq n$, ω_l and ω_u, $\underline{w}_i(\omega)$, $\overline{w}_i(\omega)$, $k_i(\omega)$ and $g_i(\omega)$ for loop-shaping weight W_i $(i = 1, 2)$. Each frequency grid-point is denoted as ω_q, where $q = 1, 2, \ldots, n_l, \ldots, n_u, \ldots, N$; ω_{n_l} and ω_{n_u} also denote ω_l and ω_u, respectively. The solution algorithm is now presented as follows:

(1) Given $\bar{\epsilon}$, find an initial controller $C_0^\star$ as a feasible starting point for the algorithm such that the interconnection $\left[W_{2,0}^\star P W_{1,0}^\star, W_{1,0}^{-1\star} C_0^\star W_{2,0}^{-1\star}\right]$ is internally stable and $b(W_{2,0}^\star P W_{1,0}^\star, W_{1,0}^{-1\star} C_0^\star W_{2,0}^{-1\star}) \geq \bar{\epsilon}$ for some $W_{1,0}^\star \in \mathscr{GH}_\infty$ and $W_{2,0}^\star \in \mathscr{GH}_\infty$. Set $i = 0$, where i denotes the iteration number, and let $\varepsilon_{max,0}^\star = -1$.
(2) Increment i by 1.
(3) (a) Solve the following quasiconvex optimization problem at each frequency grid-point $\omega_q \in [\omega_{n_l}, \omega_{n_u}]$, where $q = n_l, n_l + 1, \ldots, n_u$:
Minimize $\gamma_{\omega_q,i}^2$
such that $\exists \Lambda_{1\omega_q} \in \mathbf{\Lambda_n}, \Lambda_{2\omega_q} \in \mathbf{\Lambda_m}$
satisfying
(2c)-(2g) and the following additional constraints:
$(i)\ \theta_{i-1}^2 \Lambda_{1\omega_{n_l}} < P^*(j\omega_{n_l}) \Lambda_{2\omega_{n_l}} P(j\omega_{n_l})$ when $i > 1$,
where $\theta_{i-1} = \underline{\sigma}\left(W_{2,i-1}(j\omega_{n_l}) P(j\omega_{n_l}) W_{1,i-1}(j\omega_{n_l})\right)$,
$(ii)\ P^*(j\omega_{n_u}) \Lambda_{2\omega_{n_u}} P(j\omega_{n_u}) < \phi_{i-1}^2 \Lambda_{1\omega_{n_u}}$ when $i > 1$,
where $\phi_{i-1} = \overline{\sigma}(W_{2,i-1}(j\omega_{n_u}) P(j\omega_{n_u}) W_{1,i-1}(j\omega_{n_u}))$.
Denote by $\Lambda_{1\omega_q}^\star$ and $\Lambda_{2\omega_q}^\star$ the values of $\Lambda_{1\omega_q}$ and $\Lambda_{2\omega_q}$, respectively, that achieve the above minimization at each ω_q.
(b) Solve the following optimization problem at each frequency grid-point $\omega_q < \omega_{n_l}$ in a backward direction where $q = n_l - 1, n_l - 2, \ldots, 1$ and $\left|W_{2,i}(j\omega_q)\right|$ is pinned down to $\left(\Lambda_{2\omega_{n_l}}^\star\right)^{1/2}$ $\forall \omega_q$ (hence, $\Lambda_{2\omega_q} = \Lambda_{2\omega_{n_l}}^\star$):
Minimize $\underline{s}(\omega_q)^{-2}$
such that $\exists\ \Lambda_{1\omega_q} \in \mathbf{\Lambda_n}$
satisfying
$\Lambda_{1\omega_q} < \underline{s}(\omega_q)^{-2} P^*(j\omega_q) \Lambda_{2\omega_{n_l}}^\star P(j\omega_q)$,
(2c)-(2d) and (2f), where $\gamma_{\omega_q} = \bar{\epsilon}^{-1}$ and $\Lambda_{1\omega_{n_l}} = \Lambda_{1\omega_{n_l}}^\star$. Since the optimization is in the backward direction, $\delta\nu = \log_{10}(\omega_{q+1}) - \log_{10}(\omega_q)$, and $\Lambda_{1\omega_q}, \Lambda_{1\omega_{q-1}}$ and $g_1(\omega_q)$ are replaced by $\Lambda_{1\omega_{q+1}}, \Lambda_{1\omega_q}$ and $g_1(\omega_{q+1})$, respectively.
Denote by $\Lambda_{1\omega_q}^\star$ and $\underline{s}_i(\omega_q)^\star$ the values of $\Lambda_{1\omega_q}$ and $\left(\underline{s}(\omega_q)^{-2}\right)^{-1/2}$, respectively, that achieve the above minimization at each ω_q.

[2] The assumption that the plant has more outputs than inputs incurs no loss of generality. A dual problem to that shown in Figure 1 where $W_1 = W_2^T$, $W_2 = W_1^T$, $P = P^T$ and $C_\infty = C_\infty^T$ would be considered if the plant has strictly fewer outputs than inputs.

(c) Solve the following optimization problem at each frequency grid-point $\omega_q > \omega_{n_u}$ in a forward direction where $q = n_u+1, n_u+2, \ldots, N$ and $\left|W_{1,i}(j\omega_q)\right|$ is pinned down to $\left(\Lambda^{\star}_{1\omega_{n_u}}\right)^{-1/2}$ $\forall \omega_q$ (hence, $\Lambda_{1\omega_q} = \Lambda^{\star}_{1\omega_{n_u}}$):

Minimize $\overline{s}(\omega_q)^2$
such that $\exists\, \Lambda_{2\omega_q} \in \mathbf{\Lambda_m}$
satisfying
$P^*(j\omega_q)\Lambda_{2\omega_q}P(j\omega_q) < \overline{s}(\omega_q)^2\Lambda^{\star}_{1\omega_{n_u}}$,
(2c),(2e) and (2g), where $\gamma_{\omega_q} = \bar{\epsilon}^{-1}$ and $\Lambda_{2\omega_{n_u}} = \Lambda^{\star}_{2\omega_{n_u}}$.

Denote by $\Lambda^{\star}_{2\omega_q}$ and $\overline{s}_i(\omega_q)^{\star}$ the values of $\Lambda_{2\omega_q}$ and $\left(\overline{s}(\omega_q)^2\right)^{1/2}$, respectively, that achieve the above minimization at each ω_q.

(4) Construct *diagonal* transfer function matrices $W^{\star}_{1,i}(s)$ and $W^{\star}_{2,i}(s)$ in $\mathscr{GH}_\infty$ by fitting stable minimum phase transfer functions to each magnitude data on the main diagonal of $(\Lambda^{\star}_{1\omega_q})^{-1/2}$ and $(\Lambda^{\star}_{2\omega_q})^{1/2}$, where $q = 1, 2, \ldots, N$.

(5) Compute $b_{opt}(W^{\star}_{2,i}PW^{\star}_{1,i})$ as detailed in Glover and McFarlane [1989] and let this value be denoted by $\varepsilon^{\star}_{max,i}$. Furthermore, synthesize a controller $C^{\star}_{\infty,i}$ that achieves a robust stability margin $b(W^{\star}_{2,i}PW^{\star}_{1,i}, C^{\star}_{\infty,i}) = \varepsilon^{\star}_{max,i}$ usually using the state-space formula given in [Glover, 1984, Theorem 6.3]. Set $C^{\star}_i = W^{\star}_{1,i}C^{\star}_{\infty,i}W^{\star}_{2,i}$.

(6) Evaluate $\left|(\varepsilon^{\star}_{max,i} - \varepsilon^{\star}_{max,i-1})\right|$. If this value is very small, for instance 0.01, and has remained this small for the last few iterations, then EXIT; otherwise return to Step 2. The improvement in the loop-gain at low and high frequencies can also be used as an indicator to exit the algorithm.

The outputs from the algorithm are (i) the optimized $b(P_s, C_\infty)$ obtained in the variable $\varepsilon^{\star}_{max,i}$, (ii) the maximized $\rho_{\omega_q}(P_s, C_{\infty,i-1})$ obtained in the variable $\left(\sqrt{\gamma^2_{\omega_q,i}}\right)^{-1}$ $\forall \omega_q \in [\omega_{n_l}, \omega_{n_u}]$, (iii) smooth diagonal loop-shaping weights $W^{\star}_{1,i}(s)$ and $W^{\star}_{2,i}(s)$ that achieve $\varepsilon^{\star}_{max,i}$ and (iv) controller $C^{\star}_{\infty,i}(s)$ that achieves $b(W^{\star}_{2,i}PW^{\star}_{1,i}, C^{\star}_{\infty,i}) = \varepsilon^{\star}_{max,i}$. Being an ascent algorithm, performance and robustness at low and high frequencies, respectively, are monotonically non-decreasing as i increases.

While the optimization problems at the low and high frequency regions are solved pointwise-in-frequency, the constraints at each frequency grid-point $\omega_q \in [\omega_{n_l}, \omega_{n_u}]$ for the mid frequency optimization can be packed together into a single constraint in order to solve the optimization problem in one go. For the optimization at each grid-point, the number of decision variables is $(m + n + 2i_w)$, where $i_w = 1$ when the optimization is over only one weight and $i_w = 2$ when the optimization is over both weights. The number of decision variables therefore increases with the dimension of the nominal plant. This number does not however depend on the order of the plant.

6. NUMERICAL EXAMPLE

We consider a MIMO design example for pitch control of a highly maneuverable airplane (see Balas et al. [1994] for more information). The model is taken from the HIMAT, a scaled, remotely piloted flight model with poles and zeros located at $s = -2.2321 \pm j3.3779, -0.0442 \pm j0.2093$ and $s = -0.0226$, respectively. For the purpose of illustration of the proposed algorithm, the design objectives specified in Balas et al. [1994] are used: disturbance rejection up to 1 rad/sec in the presence of substantial plant uncertainty above 100 rad/sec and a desired closed-loop bandwidth of approximately 10 rad/sec.

In view of the above specifications, ω_l and ω_u are chosen as 12 rad/sec and 160 rad/sec, respectively. $\bar{\epsilon}$ is fixed at 0.3 for the optimization problems at low and high frequency regions, thus allowing unstructured plant perturbation $\|\Delta\|_\infty < 0.3$. The solution algorithm formulated in the previous section is now used to simultaneously synthesize weights W_1 and W_2 and a stabilizing controller C_∞. The synthesized controller using the $\mathscr{H}_\infty$ LSDP in Balas et al. [1994] with $b(P_s, C_\infty)$ of 0.4306 is used to initialize the algorithm.

W_2 is held fixed in low and mid frequencies while W_1 is held fixed in high frequencies. Due to simple design specifications, the frequency functions $\underline{w}_i, \overline{w}_i, k_i$ and g_i $(i = 1, 2)$ are chosen as $10^{-5}, 10^5, 5$ and 60 dB/dec, respectively. Two hundred equally spaced frequency points on a logarithmic scale between $\omega_1 = 10^{-2}$ rad/sec and $\omega_N = 10^4$ rad/sec are used to formulate the optimization problems in Step 3 and four iterations were required for the practical convergence of the algorithm.

For the sake of brevity, we only show the evolution of $\underline{s}(\omega_q)$ at low frequencies and $\overline{s}(\omega_q)$ at high frequencies, the corresponding loop-shaping weights and the resulting sensitivity functions in Figure 2. The first plot in Figure 2 shows that the loop-gain is maximized at low frequencies and minimized at high frequencies. Moreover, the plot of the output sensitivity function (resp. input complementary sensitivity function) is lower in low (resp. high) frequencies when compared with the design in Balas et al. [1994]. The robust stability margin obtained from this design is 0.3548, which is an indicator of a decent design. Moreover, a minimum $\rho_{\omega_q}(P_s, C_\infty)$ of 0.3680 is obtained at the mid frequency region before the final controller synthesis. The order of the synthesized loop shaping weight W_1, as well as W_2, is 13. This order can be reduced using model reduction techniques given in Zhou et al. [1996], if required. Also, the condition numbers of the weights are less than 5 at all frequencies, which is typically considered good.

7. CONCLUSION

A design paradigm that answers the question of the best achievable performance level in a feedback system has been introduced via weight optimization in $\mathscr{H}_\infty$ loop-shaping design procedure. The proposed paradigm is cast in a systematic framework that captures the design objectives in low, mid and high frequencies. Smooth loop-shaping weights and controller that maximize robust performance for a guaranteed level of robust stability margin are simultaneously synthesized from the resulting solution algorithm. The algorithm is easy to use and it gives designers a feel of what performance is achievable on a given problem.

REFERENCES

J. Balas, J. Doyle, K. Glover, A. Packard, and R. Smith. *μ-analysis and synthesis toolbox user's guide*. The MathWorks Inc., 1994.

K. Glover. All optimal hankel-norm approximations of linear multivariable systems and their $\mathscr{L}_\infty$-error bounds. *International Journal of Control*, 39(6):1115–1193, 1984.

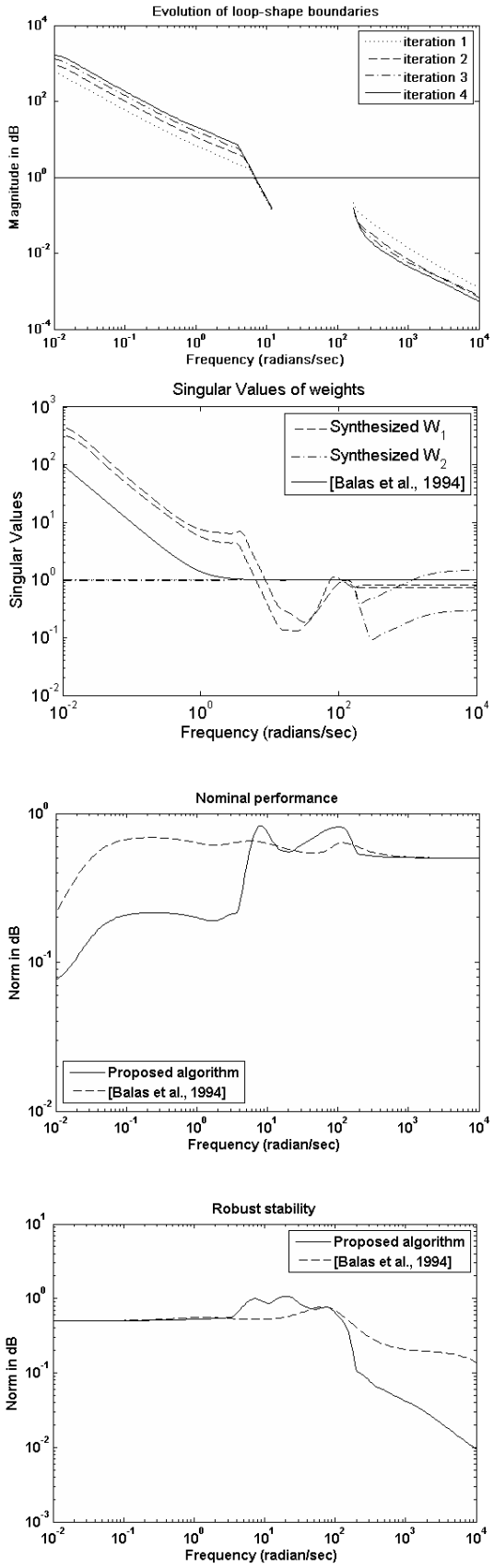

Figure 2. Loop-shape boundaries, loop-shaping weights (synthesized weights and weights from [Balas et al., 1994]), output sensitivity function and the input complementary sensitivity function

K. Glover and D. McFarlane. Robust stabilization of normalized coprime factor plant descriptions with $\mathscr{H}_\infty$-bounded uncertainty. *IEEE Transactions on Automatic Control*, 34(8): 821–830, 1989.

K. Glover, G. Vinnicombe, and G. Papageorgiou. Guaranteed multi-loop stability margins and the gap metric. *Proceedings of IEEE CDC, Sydney, Australia*, pages 4084–4085, 2000.

S. Hara, M. Kanno, and M. Onishi. Finite frequency phase property versus achievable control performance in $\mathscr{H}_\infty$ loop shaping design. *SICE-ICASE International Joint Conference, Bexco, Busan, Korea*, 2006.

R Hyde. *$\mathscr{H}_\infty$ aerospace control design-a VSTOL flight application*. In Advances in industrial control series. Berlin: Springer, 1995.

A. Lanzon. Weight optimisation in $\mathscr{H}_\infty$ loop-shaping. *Automatica*, 41(1):1201–1208, 2005.

D. McFarlane and K. Glover. A loop-shaping design procedure using $\mathscr{H}_\infty$ synthesis. *IEEE Transactions on Automatic Control*, 37(6):759–769, 1992.

B. Min, H. Ryu, D. Sang, M. Tahk, and D. Shim. *Communications in computer and information science: Advanced intelligent computing theories and applications with aspects of contemporary intelligent computing techniques. Autopilot design using hybrid PSO-SQP algorithm*, volume 2. Springer-Verlag, 2007.

M. Osinuga, S. Patra, and A. Lanzon. Incorporating smoothness into weight optimization for $\mathscr{H}_\infty$ loop-shaping design. *Proceedings of the 18th Mediterranean Conference on Control and Automation, Morocco*, pages 856–861, 2010a.

M. Osinuga, S. Patra, and A. Lanzon. Smooth weight optimization in $\mathscr{H}_\infty$ loop-shaping design. *Systems and Control Letters*, 59:663–670, 2010b.

G. Papageorgiou and K. Glover. A systematic procedure for designing non-diagonal weights to facilitate $\mathscr{H}_\infty$ loop shaping. *Proceedings of IEEE CDC, San Diego, CA, US*, pages 2127–2132, 1997.

A. Peters and M. Salgado. Performance bounds in $\mathscr{H}_\infty$ optimal control for stable siso plants with arbitrary relative degree. *IEEE Transactions on Automatic Control*, 54(8):1986–1991, 2009.

S. Skogestad and I. Postlethwaite. *Multivariable feedback control: Analysis and Design*. John Wiley and Sons, 1998.

M. Tsai, E. Geddes, and I. Postlethwaite. Pole-zero cancellations and closed-loop properties of an $\mathscr{H}_\infty$ mixed sensitivity design problem. *Proceedings of IEEE CDC, Honolulu, HI, USA*, pages 1028–1029, 1990.

G. Vinnicombe. *Uncertainty and feedback: $\mathscr{H}_\infty$ loop-shaping and v-gap metric*. Imperial College Press, 2001.

K. Zhou, J. Doyle, and K. Glover. *Robust and optimal control*. Englewood Cliffs, NJ: Prentice Hall, 1996.